Multiphase segmentation based on new signed pressure force functions and one level set function

Haider ALI[1], Noor BADSHAH[2,*], Ke CHEN[3], Gulzar Ali KHAN[1], Nosheen ZIKRIA[1]

[1]Department of Mathematics, University of Peshawar, Pakistan.

[2]Department of Basic Sciences, UET Peshawar, Pakistan.

[3]Department of Mathematical Sciences, the University of Liverpool, United Kingdom.

*Correspondence: noor2knoor@gmail.com

Abstract: In this paper we propose a new model to detect multiple objects of various intensities in images having maximum, minimum or mid-intensity background by evolving only one level set function. In this model, a new signed pressure force function based on novel generalized averages is used for segmentation of images with maximum or minimum intensity background. Although for images with mid-intensity background which are indeed challenging for 2-phase models, we propose a new product generalized signed pressure force function. Finally, to give experimental and qualitative evidence, our model is tested on both synthetic and real images with Jaccard Similarity Index. The experimental and qualitative results reveal that the proposed method is efficient in both global and selective segmentation. Our new model is also tested on colour images and the results are compared with the state of the art models.

Key words: Segmentation, Level set, Geodesic active contours, spf function

1. Introduction

Image segmentation aims to extract or distinguish objects from each other in images. In simple words, image segmentation extracts objects by distinguishing foreground and background in images [1-6]. Variational image segmentation models are categorized into two classes namely: edge based models and region based models. In edge

based models objects are extracted by capturing their boundaries while in region based models objects are detected by detecting their occupied optimal regions. For edge detection most of the models use an edge detector function which mainly depends on the gradient of a given image [4, 7, 8]. On the other hand, region based segmentation models use region detectors, named as fidelity terms, which use image statistical information to capture objects/regions [9-11]. In region based models one of the famous models is Mumford-Shah (MS) [10] which is given by:

$$F(u,K)^{MS} = \int_{\Omega} (u-u_0)^2 dxdy + \alpha^* \int_{\Omega-K} |\nabla u|^2 dxdy + \beta \int_{K} ds \quad (1)$$

where u_0 is the given image, u is the required solution and is a smooth approximation of u_0, $\alpha^*, \beta > 0$, Ω is the image domain and K is the set of edges (discontinuities) in the image. This model is theoretically very strong but computationally very complex. First variation of this model is piecewise constant MS model which consider u to be piecewise constant in each region. The level set methods [12] provided a good numerical implementation of piecewise constant (PC) MS models [5, 13] but unfortunately, for multi-region image segmentation usually multi-level set functions are evolved which are indeed time consuming approach in many situations. To enhance the performance of the PC model, Li et al. [9] proposed the local binary fitting (LBF) model by incorporating the image local statistical information in the PC model [5, 14,15]. This model may segment images with intensity in-homogeneity and gives competing results compare to the state of art models. In this model Gaussian kernel functions are used instead of average intensities. This model works well in images having intensity in-homogeneity, but computational cost is very high [16]. To overcome this drawback Wang et al. proposed local energy based model (Local Chan-Vese (LCV)) [15] which is given by:

$$F(\phi,c_1,c_2,d_1,d_2)^{LCV} = \mu\int_{\Omega}|\nabla H(\phi)|dxdy + \lambda_1\int_{\Omega}\left((u_0-c_1)^2+(u_0^{*}-u_0-d_1)^2\right)H(\phi)dxdy$$
$$+\lambda_2\int_{\Omega}\left((u_0-c_2)^2+(u_0^{*}-u_0-d_2)^2\right)\left(1-H(\phi)\right)dxdy, \quad (2)$$

where u_0^* denotes the smooth version of given image u_0 [15]. $\mu,\lambda_1,\lambda_2>0$ are trade off parameters and c_1,c_2,d_1,d_2 are average intensities of given image and difference image inside and outside level set function ϕ respectively. $H(\phi)$ is Heaviside function which is 0 if $\phi<0$ and is 1 if $\phi>0$. Similarly, Zhang et al. proposed an active contour model based on local image fitting (LIF) [16] for images with intensity in-homogeneity. Recently, Zhang et al. [16-18] combined the idea of geodesics [4] and Chan-Vese [5] model and proposed geodesic aided Chan-Vese (GCV) model as follows:

$$\frac{\partial\phi}{\partial t} = \alpha(spf).|\nabla\phi|, \ in\ \Omega, \quad (3)$$
$$\phi(t,x,y) = \phi_0(x,y), \ in\ \Omega,$$

where *spf* denotes the signed pressure force function [16-18] and $\alpha>0$. In similar connection, Akram et al. [1] modified the model in eq. (3) for images with intensity in-homogeneity by replacing the *spf* function with their local-*spf* function [1]. Although these models have improved performance of the region based active contour models, they are not designed to handle images having multiple intensity objects [16-17]. For quantitative comparison we will use the Jaccard Similarity (JS) for different models. If we denote the segmented region by R_1 and the ground truth (GT) by R_2, the JS is the ratio of the areas of the intersection by the union of the regions, i.e. $JS(R_1,R_2)=\frac{|R_1\cap R_2|}{|R_1\cup R_2|}$. For better results we want JS to be close to 1. The ground truth GT used in this paper is obtained manually in the following way: based on the maximum intensity we set a threshold value and then we choose GT as image $\leq$ threshold value. In hardware image,

the intensity values of all objects are at the most 230, we choose threshold value 240 and take GT as image ≤ 240.

In this paper, we will propose models to handle the problems discussed above. Our novel model is using a single level set function for segmentation of multi-region images having background of either maximum intensity, minimum intensity or average intensity and the objects are of homogeneous intensities. The new model is tested on both synthetic and real images. Moreover, some tests on colour images are also conducted and results are compared with a standard model.

Furthermore, for quantitative comparison of different segmentation models, the Jaccard Similarity (JS) Index [13] is presented. From experimental results, it can be seen that our proposed model perform well than the state of the art models. It can also be seen that our proposed model equally works in both global and selective segmentation.

The rest of paper is organised in the following way. In the next section some important materials and methods are discussed and the proposed model is given. In section 3 experimental results, discussions about the experiments are given. In section 4 conclusions are given.

2. The Proposed Model for Multi-region Segmentation

In 2-phase framework, the averages of the Chan-Vese (CV) model [5] consider objects of high intensities as background and objects with low intensities as foreground, so the CV and GCV models are only capable of detecting objects of either high or lower intensities. To handle this type of issues we design a new model based on generalized averages which is defined in next section. In images with maximum intensity background, we need large values of generalized averages than the CV averages to detect all the

objects. Similarly, in images with minimum intensity background, we need small values of generalized averages than the CV averages to detect all the objects.

2.1 Generalized averages in segmentation framework

Definition 1: *We define generalized averages in the following way:*

$$G_{c_1} = \frac{\int_{\Omega} {u_0}^{\beta} H(\phi)\, dxdy}{\int_{\Omega} {u_0}^{\beta-1} H(\phi)\, dxdy},\ G_{c_2} = \frac{\int_{\Omega} {u_0}^{\beta} (1-H(\phi))\, dxdy}{\int_{\Omega} {u_0}^{\beta-1} (1-H(\phi))\, dxdy}, \tag{4}$$

where β is any real number, u_0 is the given image and *H is the Heaviside function whose value is 0 if $\phi < 0$ and 1 if $\phi > 0$. The above family of averages is named as $Av-family$.*

Remark 1: The value of the parameter β should be chosen greater than 1 for images of maximum intensity background, like$\beta = 2$.For images of minimum intensity background the value of the parameter β should be chosen smaller than 1, such as $\beta = -2$. For images of mid-intensity background, it has been observed that the β and number of pixels carrying maximum intensity are proportional. Experimentally we have derived the following relation, where 0.03 is the average of ratios of β to number of pixels carrying maximum intensity:

$$\beta = 0.03 \times number\ of\ pixels\ carrying\ maximum\ intensity.$$

Now we consider the generalized averages in discrete form as

$$G_{average} = \frac{\sum_{(i,j)} u_0(i,j)^{\beta}}{\sum_{(i,j)} u_0(i,j)^{\beta-1}}. \tag{5}$$

Let's consider the following theorem for analysis.

Theorem 1: *For any positive real numbers $x_1, x_2, \ldots, x_n$ then*

(I) $\lim_{\beta\to\infty} G_{average} = Max\{x_1, x_2, ..., x_n\}$, (II) $\lim_{\beta\to-\infty} G_{average} = Min\{x_1, x_2, ..., x_n\}$.

Proof: *Let us suppose that* $x_1 \geq x_2 \geq, \ldots, \geq x_n$ *(which is possible by relabeling and combining terms together). Then*

$$\lim_{\beta\to\infty} G_{average}(x_1, x_2, ..., x_n) = \lim_{\beta\to\infty} \frac{\sum_{i=1}^{n} {x_i}^{\beta}}{\sum_{i=1}^{n} {x_i}^{\beta-1}} = \lim_{\beta\to\infty} \frac{{x_1}^{\beta} \sum_{i=1}^{n} \left(\frac{x_i}{x_1}\right)^{\beta}}{{x_1}^{\beta-1} \sum_{i=1}^{n} \left(\frac{x_i}{x_1}\right)^{\beta-1}} = x_1 = Max\{x_1, x_2, ..., x_n\}.$$

Next, to prove the second part we proceed as follows:

$$\lim_{\beta\to-\infty} G_{average} = \lim_{\beta\to-\infty} \frac{\sum_{i=1}^{n} {x_i}^{\beta}}{\sum_{i=1}^{n} {x_i}^{\beta-1}} = \lim_{\beta\to-\infty} \frac{{x_n}^{\beta} \sum_{i=1}^{n} \left(\frac{x_i}{x_n}\right)^{\beta}}{{x_n}^{\beta-1} \sum_{i=1}^{n} \left(\frac{x_i}{x_n}\right)^{\beta-1}} = x_n = Min\{x_1, x_2, ..., x_n\}.$$

This result validates that, the more β deviates from 1 in positive direction, i.e. $\beta = 2, 3, 4, 5, \ldots$, the averages deviate from the central value and tend towards maximum value of their respective data set. Similarly, the more β deviates from 1 in negative direction, i.e. $\beta = 0, -1, -2, -3, \ldots$, the averages deviate from the central value and tend towards minimum value of their respective data set. Thus we have now formulae (2) which can provide averages according to the images.

Remark: Although $G_{average}$ finds minimum and maximum value as $\beta \to -\infty$, and $\beta \to \infty$ respectively is shown mathematically in double precision but this is not the case for numerical overflows. This is given in Figure 1 (a) and (b) by taking a set of ten numbers $\{3, 5, 7, \ldots, 21\}$ and $G_{average}$ is plotted against β.

2.2 Segmenting images with minimum or maximum intensity background.

In this subsection we design a new formulation based on spf function with generalized averages to segment images having minimum or maximum intensity background. For this we define novel generalized spf function based on generalized averages as:

Definition 2: *The generalized spf function denoted by Gspf is defined as follows:*

$$Gspf_{\beta}(u_0) = \frac{u_0(x,y) - \frac{G_{c_1} + G_{c2}}{2}}{\max\left(\left|u_0(x,y) - \frac{G_{c_1} + G_{c2}}{2}\right|\right)}, \text{where } (x,y) \in \Omega. \quad (6)$$

In particular for $\beta = 1$ we have averages of the CV model [6] and consequently we have spf function of [18]. Since the quality of detection in spf based models is totally dependent on signs of a spf function and 2-phase homogeneous case is simple and can be seen in [18]. For complete detection of foreground and background in an image, Gspf function must have opposite signs in foreground and background, otherwise result will be incomplete. The signs of Gspf function depend on values of averages which are clear from equation (2) and we validate from the following tests that the types of averages which we use, matter the quality of detection. Figure 1 (c), (d), (e) and (f) illustrate that for different values of the parameter β we have different values of averages which help in capturing all multi-intensity objects in an image. The given image in this case is a maximum background image and the increment in β causes the detection of all the objects. Now we give some theoretical results for justification of proposed model.

Theorem 2: *Consider an image having q-objects with intensities $I_1, I_2, \ldots, I_q$, let I_b be the background intensity. Also let G_b and G_f be background and foreground averages. Then*

(I) *If $I_1 < I_2 <, \ldots, < I_q < I_b$ (i.e., background intensity is maximum), then for large value of β, $Gspf > 0$ in background region and $Gspf < 0$ in foreground.*

(II) *If $I_b < I_1 < I_2 <\ldots, < I_q$ (i.e., background intensity is minimum), then for large or small β, $Gspf > 0$ in foreground and $Gspf < 0$ in background region.*

Proof: *(I) For investigating the sign of $Gspf$ in background and foreground regions, we proceed as follows:*

$$\lim_{\beta\to\infty} Gspf_\beta = \lim_{\beta\to\infty} \frac{I_b - \frac{G_b+G_f}{2}}{\max\left(\left|I_b - \frac{G_b+G_f}{2}\right|\right)} = \frac{I_b - \frac{I_b+I_q}{2}}{\max\left(\left|I_b - \frac{I_b+I_q}{2}\right|\right)} > 0,$$

which means that the sign of Gspf functions positive in background region.

Next, we consider

$$\lim_{\beta\to\infty} Gspf_\beta = \lim_{\beta\to\infty} \frac{I_q - \frac{G_b+G_f}{2}}{\max\left(\left|I_q - \frac{G_b+G_f}{2}\right|\right)} = \frac{I_q - \frac{I_q+I_b}{2}}{\max\left(\left|I_q - \frac{I_q+I_b}{2}\right|\right)} < 0,$$

which means that the sign of Gspf functions negative in foreground region.

Consequently, sign of Gspf is negative in objects $I_1 < I_2 < I_3 <, \ldots, < I_{q-1}$. This means that the sign of Gspf is opposite in background and foreground. Thus by choosing a suitable large β all the objects in the image can be detected.

(II) When background has the minimum intensity and in foreground we have multi objects of different intensities. Let we have $I_b < I_1 < I_2 < I_3 <, \ldots, < I_q$.

Adopting the same approach we have

$$\lim_{\beta\to\infty} Gspf_\beta = \lim_{\beta\to\infty} \frac{I_b - \frac{G_b+G_f}{2}}{\max\left(\left|I_b - \frac{G_b+G_f}{2}\right|\right)} = \frac{I_b - \frac{I_b+I_q}{2}}{\max\left(\left|I_b - \frac{I_b+I_q}{2}\right|\right)} < 0,$$

which means that the sign of Gspf function is negative in background region.

Next, we consider

$$\lim_{\beta\to\infty} Gspf_\beta = \lim_{\beta\to\infty} \frac{I_1 - \frac{G_b+G_f}{2}}{\max\left(\left|I_1 - \frac{G_b+G_f}{2}\right|\right)} = \frac{I_1 - \frac{I_q+I_b}{2}}{\max\left(\left|I_1 - \frac{I_q+I_b}{2}\right|\right)} > 0,$$

if $I_1 > \frac{I_q + I_b}{2}$. *This means that the sign of Gspf function is positive in region with intensity* I_1. *Thus in this case sign of Gspf will be positive in the remaining objects* $I_2 < I_3 <, \ldots, < I_q$ *and consequently all the objects in foreground can be detected. But if* $I_1 < \frac{I_q + I_b}{2}$ *then we have an option to choose other suitable value of β for all objects detection in foreground because*

$$\lim_{\beta \to -\infty} Gspf_\beta = \lim_{\beta \to -\infty} \frac{I_1 - \frac{G_b + G_f}{2}}{\max\left(\left|I_1 - \frac{G_b + G_f}{2}\right|\right)} = \frac{I_1 - \frac{I_b + I_1}{2}}{\max\left(\left|I_1 - \frac{I_b + I_1}{2}\right|\right)} > 0.$$

From above theorem 2 it can be seen that images with maximum or minimum intensity background can be segmented with this formulation.

Thus we utilize Gspf function defined in equation (6) in the following manner [10]:

$$\frac{\partial \phi}{\partial t} = \alpha Gspf . |\nabla \phi|, \ in\ \Omega, \ \text{and} \qquad \phi(t, x, y) = \phi_0(x, y), \ in\ \Omega. \tag{7}$$

The above proposed partial differential equation (PDE) contains the generalized statistical image intensity information which derives the contour to the edges which truly represent the objects boundaries. For numerical solution of equation (7) we used explicit scheme in similar steps as done in [18]. Now we turn our attention towards images having background of average intensity which is indeed a challenging case for 2-phase image segmentation models. In the following section we propose a new model to tackle this serious issue.

2.3 Segmenting Images of Mid Intensity Background

Here we propose a new model for segmentation of images having mid-intensity background. For this, let we have an image containing q-objects with the following intensities: $\mathrm{I}_1 < \mathrm{I}_2 < \mathrm{I}_3 <, \ldots, < \mathrm{I}_{\mathrm{k}-1} < \mathrm{I}_\mathrm{k} = \mathrm{I}_\mathrm{b} < \mathrm{I}_{\mathrm{k}+1} <, \ldots, < \mathrm{I}_\mathrm{q}$.

Using (6) we define two functions denoted by G_B and G_F and are given by:

$$\mathrm{G_B}(u_0) = \frac{u_0(x,y) - \frac{G_{c_1}}{\theta}}{\max\left(\left|u_0(x,y) - \frac{G_{c_1}}{\theta}\right|\right)}, \quad \mathrm{G_F}(u) = \frac{u_0(x,y) - \frac{G_{c_2}}{\theta}}{\max\left(\left|u_0(x,y) - \frac{G_{c_2}}{\theta}\right|\right)}, \quad \theta > 0. \tag{8}$$

The function G_B is obtained by putting G_{c_2} equals to zero and similarly the function G_F is obtained by putting G_{c_1} equals to zero in equation (4).

For images whose background is neither of maximum nor of minimum intensity we define a new product spf function given as:

$$PGspf_{\beta,\theta} = G_B G_F. \tag{9}$$

For segmentation of images we need to have positive sign of G_B in the background and negative sign in foreground objects having intensities smaller than I_b i.e. objects having intensities $I_1, I_2, \ldots, I_{k-1}$. Similarly, we need to have negative sign of G_F in the background and positive sign in foreground objects having intensities smaller than I_b i.e. objects having intensities $I_1, I_2, \ldots, I_{k-1}$. This turns the product function $PGspf_{\beta,\theta}$ to have negative sign in background and positive sign in complete foreground in all the objects. Figure 2 exhibits a mid-intensity background image and explains the idea behind the design of the PGspf function where the aim is to get the image (PGspf function) where the background and foreground are having opposite signs. The given image u as shown in Figure 2 is the image to be segmented. The image u_1 as shown in Figure 2 is the first image which is obtained by subtracting $\frac{I_q}{\theta}$ from the given image, where I_q denotes the maximum intensity and for this particular image $\theta \in (1, 2.5)$ is a parameter and in this

case we can take 2.1. Next, the image u_2 is the image shown in Figure 2 and it can be easily seen that the sign of the background and foreground are opposite.

Now to obtain the desired results from G_B and G_F we establish bounds on parameter θ. Mathematically, we have the following constraints on θ:

$$I_b - \frac{I_b}{\theta} > 0, \quad I_q - \frac{I_q}{\theta} > 0, \quad I_b - \frac{I_q}{\theta} > 0.$$

From first two inequalities we get the lower bound $1 < \theta$ and from the third, the upper bound $\theta < \frac{I_q}{I_b}$. Thus the parameter θ exists and its value lies in the interval $1 < \theta < \frac{I_q}{I_b}$.

Thus, base on $PGspf_{\beta,\theta}$ we consider the following evolution problem:

$$\frac{\partial \phi}{\partial t} = \alpha \mathrm{PGspf}_{\beta,\theta} .|\nabla \phi|, \ in\ \Omega, \quad \text{where } \phi(t,x,y) = \phi_0(x,y), \ \text{in } \Omega. \qquad (10)$$

For numerical solution we use explicit scheme in similar steps as done in [18].

The overall algorithm can be described in the following steps:

1. Initialize the level set function ϕ as binary function.
2. Evolve the level set function ϕ according to equation (7) if an image is either of maximum or minimum intensity background and evolve it according to (10) if image is of mid-intensity background (we solve equation (7) and (10) explicitly).
3. Smooth the function ϕ by Gaussian kernel i.e. $\phi = G_\sigma * \phi$, where σ is the standard deviation.
4. Check whether the evolution is stationary. If not, return to step 2.

For segmentation of **colour images** the above algorithm is applied on each channel (R, G and B) of the image separately.

In next section we give some experimental results of the proposed model and some state of the art models.

3. Numerical Experiments

In this section, we give experimental results of the proposed generalized signed pressure function based (GSF) model and compare its results with the state of art models like GCV [18], local Chan-Vese (LCV) model [15] and locally computed spf (LCS) model [1]. From the experimental results it can be seen that our proposed method perform efficiently in images having maximum, minimum or mid-intensity background.

Performance of the proposed model in noisy images

In Figure 3, proposed method is tested on a noisy image. In Figure 3 (a) Original noisy satellite image is given and in Figure 3(b) final result of the proposed GSF model is given. Figure 3(c) displays a multi-region noisy synthetic image and Figure 3(d) shows the successful detection by the GSF model. So we conclude that our proposed model works very well in noisy images. In Figure 4, experimental results of all four models are given on an aeroplane image.

Comparison of the four models in images of minimum intensity background

In Figure 5 proposed model performance on saw image having multi intensity region and minimum intensity background is compared with LCV, GCV and LCS. Better performance of our proposed model can be seen in the experimental results and also verified by Jaccard similarity values.

Comparison of all models on image with maximum intensity background

In Figure 6, all the four models are tested on a real hardware image, which has maximum intensity background and in-homogeneity in its foreground. Our proposed method has performed very well in this type of images, while the other methods fail to segment this image. For comparison JS values for our proposed model is 1.

Comparison of all models on image with mid-intensity background

The four models are tested on a real multi-objects image containing a bird and moon and having mid-intensity background which is given in Figure 7. Our proposed model performed has detected both objects in the image while the other models GCV, LCV and LCS models could detect both objects. JS value for our model is 0.9.

Selective segmentation results of the proposed model

For selective image segmentation GCV and GSF are tested on the image given in Figure 8 where the initial contour encloses the kidney to be captured. The GCV model detected the kidney with undesirable region whereas the GSF model captured purely the kidney of interest without any undesirable result. Next, it can be easily observed that the proposed GSF model captured the true boundaries of internal structure of given brain CT image whereas the result by the GCV model can also be seen. JS values are given for comparison.

Performance of the GSF model in colour images

To exhibit the performance of the proposed model on colour images, firstly, the proposed GSF model and the vector valued Chan-Vese (VVCV) model [5, 12] are tested on colour images having multi intensity objects as in Figure 9. It can be very easily observed from these figures that the GSF model captured successfully all the different intensity objects completely in contrast with the standard VVCV model. Similarly, Figure 9 displays an aeroplane in inhomogeneous intensity sky. The proposed GSF model successfully detected the aeroplane in contrast with the VVCV model.

Speed comparison of all four models

Next, using image in Figure 3(a), the time comparisons of all four models is given in Table 1. These experiments are done by using MATLAB 7.11.0, with Windows 7, 2.53GHz Intel Core i3 personal computer with 2GB RAM. The following notations are

used in Table1; Size: the size of given image $m \times$ n, Iter: total number of iterations, CPU: the CPU time in seconds. From the table it can be seen that our model is as fast as GCV, because in both models we are solving same partial differential equation, but we are using different spf function. LCV is fast in time but its performance is limited in the above discussed problems. In Table 2, quantitative comparison of different models in terms of (mean$\pm$SD) of JS values is given, where SD is the standard deviation. For JS values comparison we have used synthetic images with maximum, minimum and mid intensity backgrounds like images given in Figures 1, 2, 5, 6, 7. It can be observed that our proposed model gives better JS values in different problems.

4. Conclusion

In this paper we have proposed a novel active contour model based on generalized averages and spf functions for segmenting images that have multi-objects, having either maximum, minimum or mid-intensity backgrounds. For images with constant intensities, all the four state of the art models work well but images having multi-regions can only be segmented by our proposed GSF model which can be seen from the experiments. However, images in which objects have intensity in-homogeneity may not be segmented efficiently by proposed algorithm which is our future task.

5. References

[1] Akram F, Kim J, Lim H, Choi K. Segmentation of intensity inhomogeneous brain MR images using active contours. Comput. Math. Methods in Med 2014; 2014: 1—14.

[2] Ali H, Badshah N, Chen K, Khan GA. A variational model with hybrid images data fitting energies for segmentation of images with intensity inhomogeneity. Pattern. Recogn 2016; 51:27—42.

[3] Badshah N, Chen K, Ali H, Murtaza G. Coefficient of variation based image selective segmentation using active contour. East Asian J Appl Math 2012; 2: 150—169.

[4] Caselles V, Kimmel R, Sapiro G. Geodesic active contours. Int. J Comput Vision 1997; 22:61—79.

[5] Chan T, Vese L. Active contours without edges. IEEE T Image Process 2001; 10:266—277.

[6] Chen K. Matrix preconditioning Techniques and Applications. 1st Ed. The Edinburgh Building, Cambridge CB22RU, UK: Cambridge University Press, 2005.

[7] Guyader C, Gout C. Geodesic active contour under geometrical conditions theory and 3D applications. Numer. Algorithm 2008; 48: 105—133.

[8] Kass M, Witkin A, Terzopoulos D. Active contours models. Int J Comput Vision 1988; 1:321—331.

[9] Li C, Kao C, Gore J, Ding Z. Implicit active contours driven by local binary fitting energy. In: Proceedings of IEEE conference on Computer Vision and Pattern Recog (CVPR) 2007; pp.1—7.

[10] Mumford D, Shah J. Optimal approximation by piecewise smooth functions and associated variational problems. Commun Pure Appl. Math 1989; 42:577—685.

[11] Murtaza G, Ali H, Badshah N. A robust local model for segmentation based on coefficient of variation. J Inf Commun Technol2011; 5:30—39.

[12] Osher S, Fedkiw R. Γ-Level set methods and dynamic implicit surfaces, springer Verlag. 2003; Lec Notes Comp Sci 2005; 3708:499—506.

[13] Chan TF, Sandberg BY, Vese LA. Active contour without edges for vector valued Images. J Vis Commun and Image R 2000; 11: 130—140.

[14] Vese LA, Chan TF. A multiphase level set framework for image segmentation using the Mumford and Shah Model. Int J Comput Vision 2002; 50:271—293.

[15] Wang X, Huang D, Xu H. An efficient local Chan-Vese model for image segmentation. Pattern. Recogn 2010; 43:603—618.

[16] Zhang K, Song H, Zhang L. Active contours driven by local image fitting energy. Pattern. Recogn 2010; 43:1199—1206.

[17] Zhang C, Zhang Y, Lin Z. Automatic face segmentation based on the level set method. In: National Conference on Information Technology and Computer Science; 16-18 November 2012; Lanzhou, China. pp. 678—681.

[18] Zhang K, Zhang L, Song H, Zhou W. Active contours with selective local or global segmentation: A new formulation and level set method. Imag Vision Comput 2010; 28:668—676.

Figures:

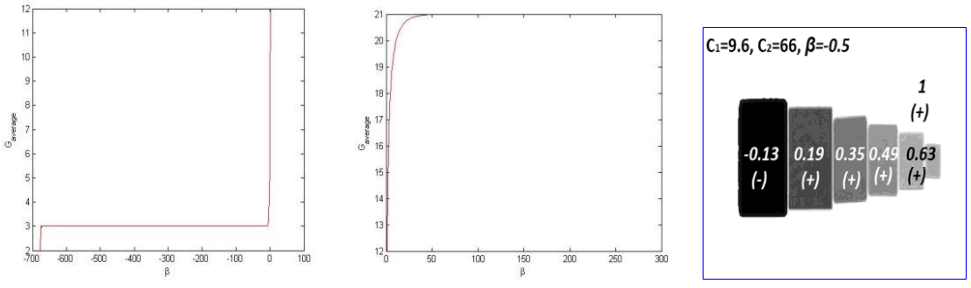

(a) (b) (c)

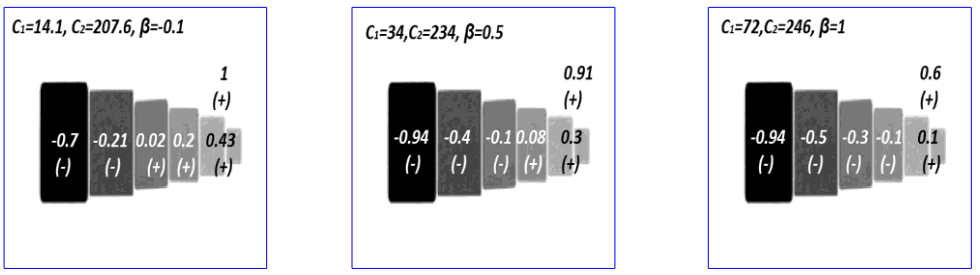

(d) (e) (f)

Figure 1: In (a) and (b) numerical overflow is given for $\beta < -679$ and $\beta > 233$ for a set of values $\{3, 5, \ldots, 21\}$ and $G_{average} \to -\infty, \infty$ respectively. And in (c), (d), (e) and (f) signs of Gspf function inside and outside of the object for different values of averages. Clearly the above figures illustrate that a single pair of averages may not help in obtaining the desired result of segmentation. The suitable value of parameter β helps us in obtaining a suitable pair of averages from the *Av-family*.

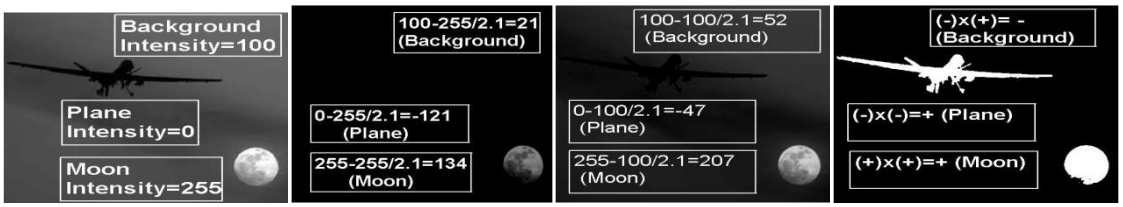

(a) (b) (c) (d)

Figure 2: Illustration of the $PGspf_{\beta,\theta}$ function in segmenting real image having mid-intensity backgroundwhere maximum intensity (I_q) is 255, background intensity (I_b) is 100 and choosing θ in interval (1, $\frac{I_q}{I_b}$=2.5). (a) Given Image u; (b) Image $u_1 = u - \frac{I_q}{\theta}$; (c) Image $u_2 = u - \frac{I_b}{\theta}$; (d) The product image $u_1 \times u_2$ where $\theta = 2.1$.

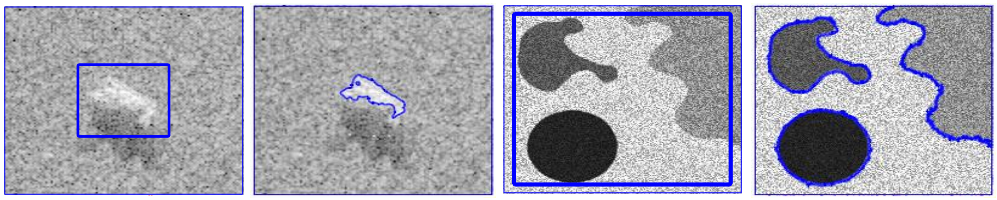

(a) (b) (c) (d)

Figure 3: Performance of the GSF model in segmenting real noisy satellite image and a multi region synthetic noisy image. (a) Real noisy satellite image; (b) Result by the GSF model, $\beta = 2, \mu = 10, \text{iterations} = 100$; (c) Multi region synthetic noisy image; (d) Result by the GSF model, $\beta = 1.5, \mu = 13, iterations = 250,\ size(u) = 200 \times 200$.

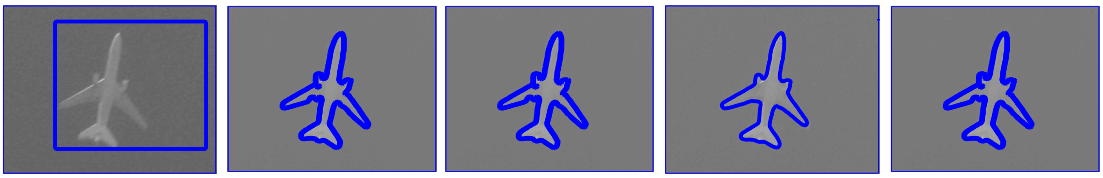

(a) Initial guess (b) GCV Result (c) LCV Result (d) LCS Result (e)GSF Result

Figure 4: Experimental test exhibiting that all the four models work well in simple image.

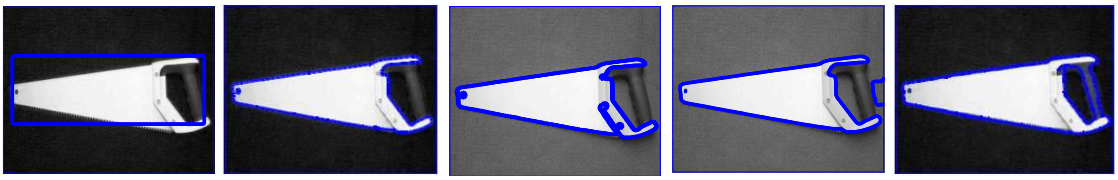

(a) Initial guess (b) GCV Result (c) LCV Result (d) LCS Result (e) GSF Result

Figure 5: Segmenting a real hardware image having minimum intensity background. GCV (JS=0.78), LCV (JS=0.79), LCS (JS=0.7),GSF(JS=0.88). For proposed model parameters used are:$\beta = -0.906, \mu = 77, iter = 65, size(u) = 200 \times 200$.

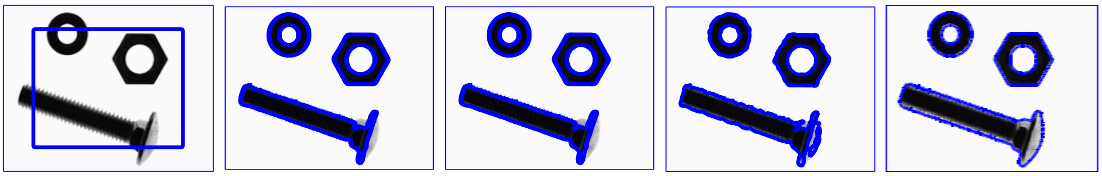

(a) Initial guess (b) GCV Result (c) LCV Result (d) LCS Result (e) GSF Result

Figure 6: Segmenting a real hardware image having maximum intensity background.GCV (JS=0.8), LCV (JS=0.8), LCS (JS=0.85),GSF model (JS=1). For proposed model parameters used are:$\beta = 3, \mu = 15, iter = 100$.

(a) Initial guess (b) GCV Result (c) LCV Result (d) LCS Result (e) GSF Result

Figure 7: Segmenting a real world image having background intensity neither maximum nor minimum. GCV (JS=0.48), LCV (JS=0.48), LCS (JS=0.1), GSF(JS=0.9). For proposed model parameters used are:$\beta = 3, \mu = 40, iter = 120, \theta = 4$.

(a) (b) (c)

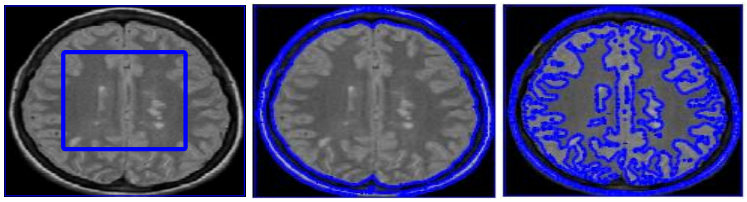

(d) (e) (f)

Figure 8: Testing performance of the two models in single and multiple organ segmentation using real medical images. (a) Object of interest; (b) GCV Result (JS=0.992); (c) GSF (JS=0.996). (d) Object of interest;(e) GCV Result (JS=0.6); (f) GSF Result (JS=0.8). For GSF parameters are: $\beta = 2, \mu = 5$ *(a)*, $\beta = 2, \mu = 15$.

(a) (b) (c)

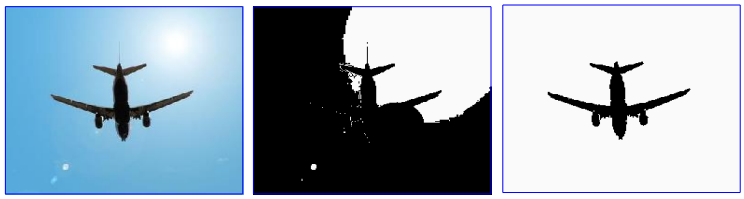

(d) (e) (f)

Figure 9: Testing performance of the GSF and vector valued CV (VVCV) model.For (a) VVCV (JS=0.81), GSF (JS=0.996), for (d) VVCV (JS=0.5), GSF (JS=0.992). For GSF parameters used are: $\beta = 5, \mu = 20, iter = 100$ *for (a); and* $\beta = 0.5, \mu = 10, iter = 100$ for (d).

Tabels:

Size	GSF		GCV Method		LCV Method		LCS Method	
	Iter	CPU	Iter	CPU	Iter	CPU	Iter	CPU
200× 200	17	0.4	17	0.4	2	0.3	62	3.4
400× 400	50	3	50	3	2	0.7	166	36
600× 600	80	17	80	17	2	2	290	208
800× 800	110	31	110	31	2	2.6	430	498

Table.1: CPU time comparison of the LCV, GCV, LCS and our proposed GSF model.

Intensity	GCV Model	LCV Model	LCS Model	GSF Model
Maximum	0.68±0.1	0.6±0.1	0.88±0.03	0.98±0.02
Minimum	0.73±0.04	0.8±0.11	0.8±0.1	0.96±0.02
Mid	0.57±0.2	0.53±0.2	0.5±0.3	0.93±0.03

Table.2: Mean and the SD of JS values for state of art models tested on images with diffferent intesity backgrounds.